

Analysis of deposit behaviour in crossflow microfiltration by means of thickness measurement

Mourad Hamachi^a, Martine Mietton-Peuchot^{b,*}

^a *Laboratoire de Génie Chimique CNRS/UMR 5503, 18 Chemin de la loge, 31078 Toulouse, France*

^b *Université victor Segalen Bordeaux 2, 351 cours de la libération, 33405 Talence Cedex, France*

Received in revised form 20 April 2001; accepted 9 May 2001

Abstract

Deposit build-up is the most serious constraint in crossflow microfiltration processes since it leads to a significant decrease in permeate flux. Therefore, controlling deposit build-up is necessary for membrane process optimisation. The use of a model suspension of clay (bentonite) and an optical measurement technique for deposit thickness makes it possible to characterise the properties of the deposit and the conditions under which it builds-up. This study investigates the relationship between permeate flux and the filtration conditions affecting the deposit build-up. It shows that for specific operating conditions, permeate flux can be stabilised and that cake formation is substantially avoided. For the highest crossflow velocity tested, 88% of the mass carried by convection to the membrane surface is swept away by the tangential flow. © 2002 Elsevier Science B.V. All rights reserved.

Keywords: Microfiltration; Fouling; Membrane; Critical flux; Deposit thickness

1. Introduction

Amongst the membrane processes, crossflow microfiltration and ultrafiltration are the most widely used at an industrial level. The nature of products to be filtered by these techniques can vary greatly according to their applications. Crossflow microfiltration targets suspensions of micronic particles, but these are rarely found alone in the suspension. These particles of micron size are situated in an ambiguous border area where purely hydrodynamic phenomena are observed, but where physico-chemical phenomena also compete for the process control. The low hydraulic resistance of the membranes used leads to lower pressures than in ultrafiltration and to a greater permeate flux. To achieve a higher permeate flux, it is common to increase crossflow velocity. This requires extra energy or an increase in transmembrane pressure, thus, leading to a quick deposit build-up which may induce irreversible fouling. Backflush washing or regeneration of membranes are also used but this means that the filtration process is temporarily off-line. Recent research has reported that high initial fluxes lead to more fouling than lower fluxes.

The crossflow velocities used generally ensure a turbulent regime in the filtration module. Nevertheless, this does not avoid all fouling either within or at the surface of the membrane. Thus, the control of deposit build-up is crucial for the optimisation of membrane plants.

In the present paper, the measurement of deposit thickness is used to study the various relationships between deposit build-up and the parameters of filtration.

2. Materials and methods

2.1. Crossflow microfiltration equipment and procedures

The experiments were conducted with a classic pilot crossflow filtration loop fitted for the measurement of deposit thickness (Fig. 1).

The suspension was sent through the filtration loop by a centrifugal pump. The circulation flow rate was measured by the flowmeter and the transmembrane pressure was set up by the gradual closure of the two gates V1 or V2 or both at once. Effective pressure was taken as being equal to the average pressure values upstream and downstream of the module. The temperature of the suspension was regulated by the heat exchanger and all experiments were conducted at a temperature of 20 ± 2 °C. The suspension flowed from the inlet at the bottom of the module and was extracted at the

* Corresponding author. Tel.: +33-05-5684-6495;

fax: +33-05-5684-6468.

E-mail address: martine.mietton-peuchot@u-bordeaux2.fr (M. Mietton-Peuchot).

Nomenclature

B	deposit permeability (m^2)
c	suspension concentration (Kg m^{-3})
d_g	sauter diameter (m)
D_s	shear-induced diffusion coefficient ($\text{m}^2 \text{s}^{-1}$)
$e p_g$	deposit thickness (m)
h_k	Carman Kozeny constant
J	permeate flux ($\text{m}^3 \text{h}^{-1} \text{m}^{-2}$)
l	membrane length (m)
M_c	material mass carried by convection (Kg)
M_g	deposit mass (Kg)
n	acquisition point number
R	membrane radius (m)
S_m	membrane surface (m^2)
u	crossflow velocity (m s^{-1})
U_L	lift velocity (m s^{-1})

Greek letters

ΔM	mass of particles swept away (Kg)
ΔP	transmembrane pressure (kPa)
Δt	acquisition timeslot (s)
ε	deposit porosity
ρ_b	density of swollen bentonite (Kg m^{-3})

top to avoid particle sedimentation. The module consisted of one tubular mineral membrane corresponding to a filtration area of 146 cm^2 .

The membrane manufactured by SCT-US Filter (France) has an external alumina skin with a nominal pore size of $0.2 \mu\text{m}$.

Before any experiment, the membrane was immersed in an ultrasonic tank with distilled water for 10 min. This procedure reproduced roughly the same water permeation flux as found with a new membrane or one that has been cleaned

using the standard nitric acid/water/caustic cycle used to regenerate fouled membranes.

The microfiltration experiments were carried out with a bentonite suspension (Volclay SPV). The latter was prepared with distilled water filtered at $30 \mu\text{m}$ for 24 h before the experiment to avoid any variation in particle size due to hydration. A grain-size distribution analysis identified a range of particle sizes from 0.77 to $7.54 \mu\text{m}$ with a mean diameter of $2.45 \mu\text{m}$. Therefore, all these particles could be caught in the retentate stream and the only fouling which could occur was the deposit at the membrane surface. The suspension maintained the same granulometric range (average diameter of $2.57 \mu\text{m}$) over time in the filtration cycle, the bentonite particles being unaffected by the pumping process. Even if the permeate was not continuously recycled, the concentration of the retentate could be considered as constant since the variation in volume did not exceed 5% during the experiment. The mass of deposit was compared to the solids inventory through Eq. (4). For the maximum deposit thickness ($550 \mu\text{m}$), the variation in concentration was 5.6%.

The concentration of the suspension was set between 0.05 and 0.375 g l^{-1} and the average crossflow velocities were in the range from 0.05 to 0.55 m s^{-1} . The transmembrane pressures used were 110 , 160 and 210 kPa , i.e. the kind of pressures usually encountered in water treatment.

2.2. Deposit thickness measurement

The principle deposit thickness measurement was based on the tangential focusing of an He–Ne laser beam onto the membrane surface [1]. The image of the focal point was then picked up on a photomultiplier, thus, allowing immediate measurement of the signal. The build-up of a deposit on the membrane surface was expressed as an absorption of light, and this variation in signal intensity corresponded directly to the deposit thickness through a calibration curve recorded at the beginning of the experiment. This calibration curve was used to link signal fading to the displacement of the membrane; during deposit formation, it was, thus, assumed that deposit thickness was equivalent to displacement. By comparing each experimental value of the signal to the calibration curve, deposit thickness could continuously be determined.

3. Results and discussion

Fig. 2 shows the evolution over time of permeate flux and deposit thickness, at a constant pressure and concentration. In all cases, a very quick decrease in permeate flux at the start of the process was followed by a quasi-linear increase in deposit thickness.

The deposit build-up and the variation in initial permeate flux differed little, whatever the crossflow velocity. This confirms the observations of several authors that the start of the process is governed by a purely frontal filtration rate

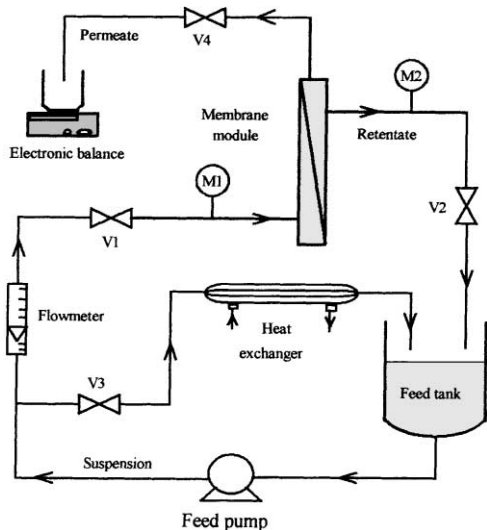


Fig. 1. Filtration pilot (M1, M2: manometers; V1–V4: regulating gates).

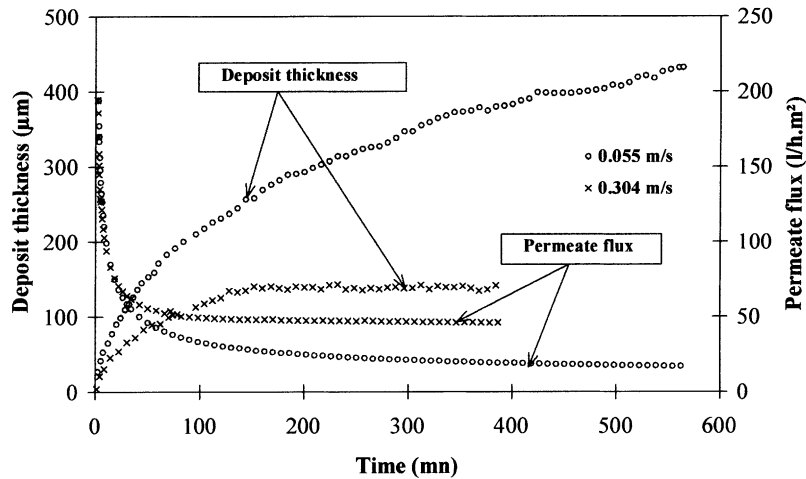


Fig. 2. Deposit thickness and permeate flux evolution ($\Delta P = 210 \text{ kPa}$, $c = 0.25 \text{ g l}^{-1}$).

[2]. This initial phenomenon is due to the large amount of particles deposited at the membrane surface. During this initial period, only a few particles are swept away because the permeate flux is perpendicular to the tangential flow. For a short time, the crossflow velocity, therefore, has very little effect on the deposit build-up.

Even though the deposit thickness is reduced and the permeate flux is increased with growing crossflow velocity, this is little information to date regarding the preferential mode of action of crossflow velocity either on permeate flux or on deposit thickness, when these are considered individually. The investigation of permeate flux as a function of deposit thickness reveals the particular effects of crossflow velocity.

Fig. 3 shows that same deposit thickness gave a lower flux at higher velocity, and that the same flux lead to a thinner deposit at a higher velocity. This is due to particle classification, i.e. particles are smaller in the cake at higher velocity. This may be attributed to the inertial lift velocity ($U_L \propto d_p^3$)

[3,4] or to the shear-induced diffusivity ($D_s \propto d_p^2$) [5,6]. Therefore, small particles are more likely to be deposited on the cake layer than bigger ones. This yields a high specific resistance and suggests that there must be an optimal velocity, which it is pointless to exceed.

It is to be noted that, whatever the velocities, the curve stabilises at a specific point (permeate flux and deposit thickness each tending towards a particular limit). These specific points plotted for different transmembrane pressures in Fig. 4 show that when pressure increases, the deposit thickness increases, for the same flux at equilibrium. This leads to the conclusion that an increase in deposit thickness offsets the increased transmembrane pressure. Thus, in the range of pressures studied and at a given concentration, crossflow velocity is the only factor governing the stationary state of the permeate flux (an observation that differs from those of Hoogland et al. [7]). In other words, beyond a certain value, increasing the transmembrane pressure will only result in

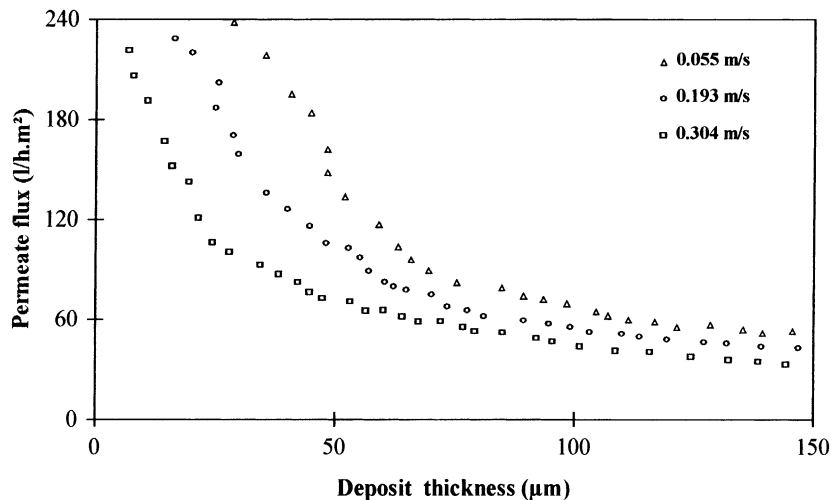


Fig. 3. Evolution of permeate flux vs. deposit thickness ($\Delta P = 110 \text{ kPa}$, $c = 0.375 \text{ g l}^{-1}$).

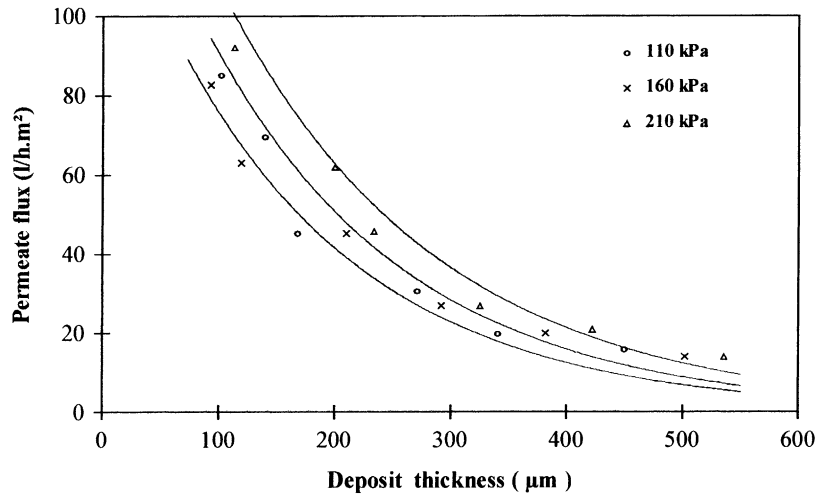


Fig. 4. Attainable permeate flux value for the membrane used ($c = 0.375 \text{ g l}^{-1}$).

increased energy consumption for the same permeate flux at the equilibrium state. Even if the thickness/permeate flux field is widened, the influence of transmembrane pressure on permeate flux can only be felt in the transient regime, in which the deposit continues to build-up.

When the deposit thickness tends to zero, the extension of the curves seems to lean towards values which are lesser than the water flux of the membrane ($3 \text{ m}^3 \text{ h}^{-1} \text{ m}^{-2}$). This may be attributed to the variation in the deposit structure.

Starting with an equilibrium state which is reached at a low crossflow velocity, an increase in crossflow velocity (Fig. 5) leads to a decrease in deposit thickness, and thus, an increase in permeate flux. This increases to reach the stable value achieved for the same velocity in other experiments conducted with a constant velocity and no disturbance during the experiment. This suggests that the deposit is reversible.

When the permeate flux was adjusted to a value corresponding to the final equilibrium (Fig. 6) by partially closing

the permeate gate V4, deposit build-up was limited to about $10 \mu\text{m}$. Indeed, the flux remained nearly unchanged throughout the experiment after a small initial drop. This agrees with recent studies reporting the existence of a critical flux below which there is no fouling [8–10]. The small initial decline in filtrate flux may be explained by the quasi-instantaneous appearance of the narrow layer of particles. In this case, the critical flux is equal to the limiting flux, which is reached after a deposit thickness of about $165 \mu\text{m}$. Even if the thickness of the deposit remains constant, the limiting flux continues to decline because the deposit is being fouled by the fine particles.

Therefore, the adjustment of filtrate flux at the start of filtration is of interest in industrial applications to limit deposit build-up. In fact, this approach makes it possible to optimise and to control the back flushing frequency of membranes, thus, lengthening times that membranes stay operational. Even more importantly, as the filtrate flux maintains

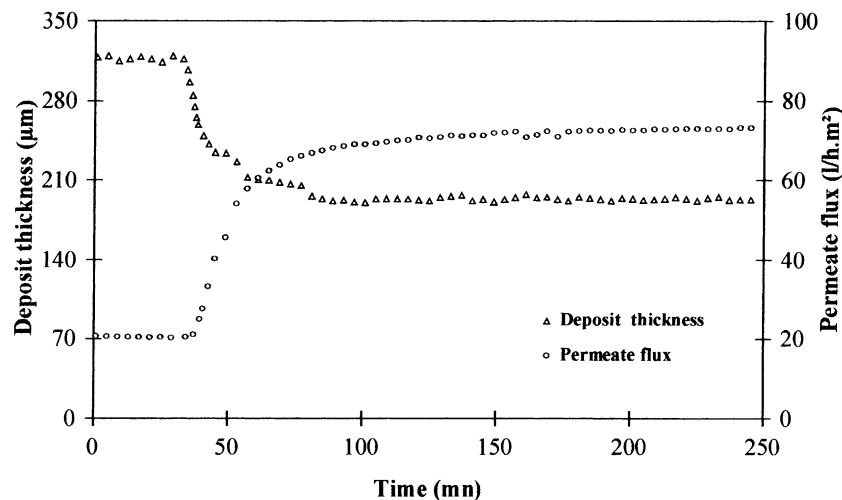


Fig. 5. Effect of increasing crossflow velocity to 0.414 m s^{-1} starting from a state of equilibrium reached at 0.11 m s^{-1} ($\Delta P = 160 \text{ kPa}$, $c = 0.25 \text{ g l}^{-1}$).

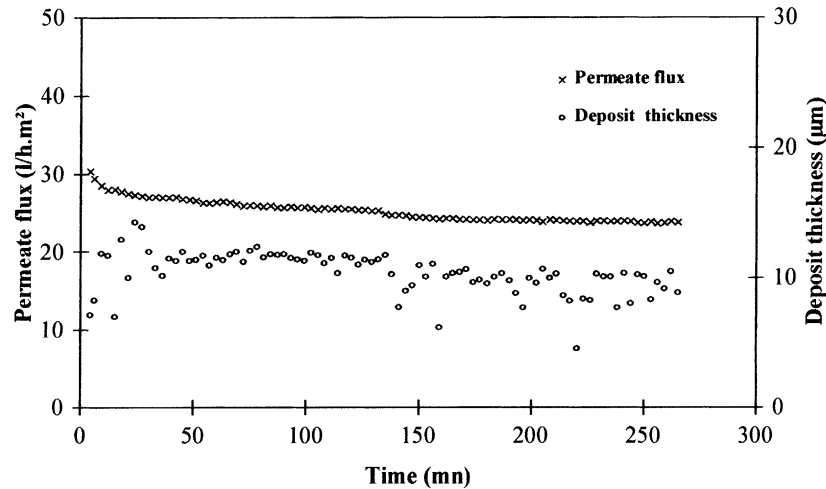


Fig. 6. Adjustment of the initial permeate flux at $30 \text{ l h}^{-1} \text{ m}^{-2}$ ($u = 0.3 \text{ m s}^{-1}$, $\Delta P = 110 \text{ kPa}$, $c = 0.375 \text{ g l}^{-1}$).

a constant value, the process may be operated continuously with no variation in permeate quality over time.

Fig. 6 shows that most of the deposited material on the membrane was closely linked to the convective flux, given that the filtrate flux in the transient phase was high. Thus, to limit fouling phenomena, one must shorten and control the transient phase.

3.1. Evaluation of particle mass swept away

Increasing crossflow velocity makes it possible to reduce deposit build-up. This suggests that the crossflow velocity restores to the tangential flow those particles which are accumulated at the membrane surface. In other words, the amount of material swept away is the determining factor to control the deposit. Therefore, we undertook to assess the re-entrained material, i.e. the de-fouling of the membrane through increased crossflow velocity. To carry out such an evaluation, we calculated on the one hand the mass of material carried by convection (M_c) to the membrane surface, and on the other hand, the mass of the deposit (M_g).

Mass of material carried by convection:

$$M_c = \int_0^t J(t)cS_m dt \quad (1)$$

where $J(t)$ is the instantaneous permeate flux.

Since the timeslot for data acquisition is very short (1 min), the integral may be approximated by a summation of the data acquisition:

$$M_c = \sum_{i=1}^n J_i c \Delta t S_m \quad (2)$$

The mass of particles swept away (ΔM) is, thus, the difference between the mass carried by convection and that present in the cake.

$$\Delta M = M_c - M_g \quad (3)$$

$$\text{Deposit mass} : M_g \pi e p_g l (e p_g + 2R)(1 - \varepsilon) \rho_b \quad (4)$$

Since the thickness of the cake and the permeate flux are measured simultaneously, the porosity is determined using the Carman Kozeny equation.

$$B = \frac{1}{36 h_k} \frac{d_g^2 \varepsilon^2}{(1 - \varepsilon)^2} \quad (5)$$

The average porosity of the deposit is about 10% [11].

The Eq. (2) used to calculate the mass provided by convection to the membrane surface gives the dry mass of the bentonite. Conversely, Eq. (4) as written provides the mass of swollen bentonite. Therefore, in order to calculate the mass of particles swept away through the relationship (3), the two masses must be expressed similarly. To do this, one must substitute the density ρ_b in the Eq. (4) by the mass of dry bentonite contained in a volume unit of swollen bentonite.

The volume of wet bentonite SPV particles is 15 times greater than that of dry particles; by knowing the average diameter of swollen particles (through granulometric analysis) as well as the volumic mass of dry bentonite, the mass of dry bentonite contained in a litre of wet bentonite can be set at 247.33 g. This makes it possible to calculate the mass of particles swept away during a filtration experiment.

Table 1 shows the overall mass of particles swept away as a function of crossflow velocity. It shows that increased velocities are helpful in reducing the mass of material

Table 1
Mass of particles swept away by the tangential flow

	$c = 0.25 \text{ g l}^{-1}$				
	$\Delta P = 110 \text{ kPa}$				
u (m/s)	0.055	0.193	0.304	0.414	0.552
M_c (g)	1.65	1.015	0.957	1.217	1.658
M_g (g)	1.40	0.55	0.35	0.29	0.19
ΔM (g)	0.24	0.46	0.60	0.92	1.45
M (%)	14.91	45.66	63.05	75.74	87.96

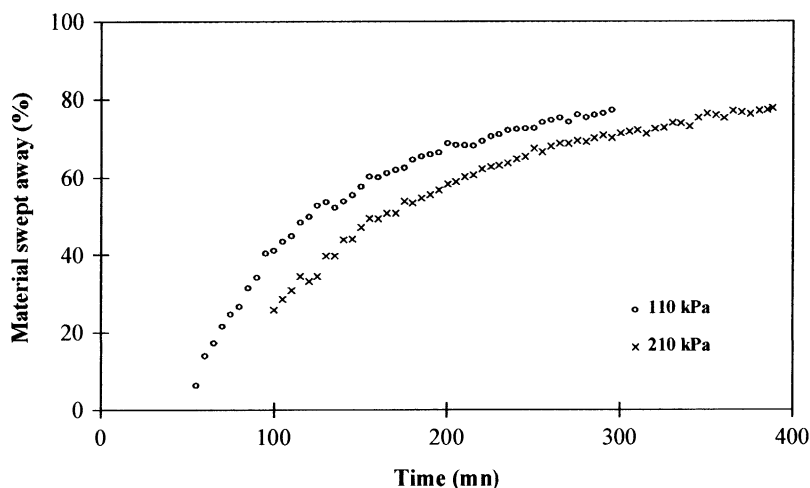


Fig. 7. Percentage of material swept away vs. time ($u = 0.414 \text{ m s}^{-1}$, $c = 0.25 \text{ g l}^{-1}$).

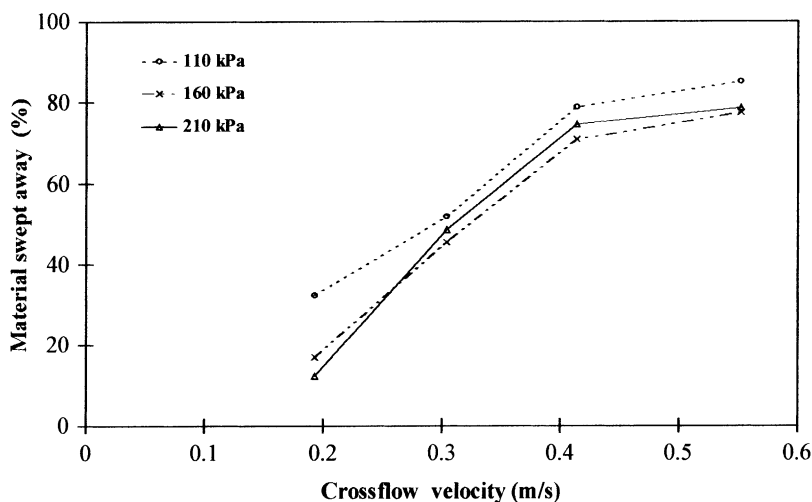


Fig. 8. Percentage of material swept away vs. crossflow velocity ($c = 0.375 \text{ g l}^{-1}$).

deposited on the membrane surface. In certain cases, 88% of mass was carried away at the highest velocity tested. These results justify increasing velocity as a method of increasing filtrate flux.

Fig. 7 shows that the proportion of particle mass swept away increases over time, finally reaching a limit of around 80% for a velocity of 0.414 m s^{-1} , whatever the pressure. This upper limit is explained by the fact that the maximum rate for particles instantaneously swept away is 100%, given the stabilisation of the deposit thickness and the permeate flux.

Pressure increase slows down the re-entrained particles, owing to the extent of convection forces, which tend to plaster the particles to the membrane surface. This means that the deposit thickness becomes ever greater as pressure increases.

The influence of crossflow velocity on overall mass of particles swept away (Fig. 8) shows that an increase in velocity results in more and more particles being re-entrained

until a velocity of 0.414 m s^{-1} is attained. Afterwards, the mass becomes more stable.

4. Conclusion

This study of the effect of filtration parameters on deposit thickness and permeate flux shows that at the start of filtration, the crossflow velocity has little effect on deposit build-up and that an increase in transmembrane pressure offsets the deposit growth for the same permeate flux. Calculation of the overall particle mass swept away with this bentonite suspension and in those conditions of study shows that up to 88% of the mass of material carried by convection on the membrane surface can be re-entrained.

Therefore, to improve the permeate flux limit, it is essential to act on the initial transitory filtration period, since the re-entrainment of particles remains limited, unlike when a

state of equilibrium is reached. In certain operating conditions, filtrate flux may be stabilised and superficial fouling avoided.

References

- [1] M. Hamachi, M. Mietton Peuchot, Cake thickness measurement with an optical laser sensor, *Chem. Eng. Res. Design* 79 (2001) 151–155.
- [2] S. Nakao, S. Namura, S. Kimura, Transport phenomena of the crossflow microfiltration process, in: *Proceedings of the Fifth World Filtration Congress*, Nice, France, 1990, pp. 295–307.
- [3] F.W. Altena, G. Belfort, Lateral migration of spherical particles in porous flow channels: application to membrane filtration, *Chem. Eng. Sci.* 39 (2) (1984) 343–355.
- [4] G. Green, G. Belfort, Fouling of ultrafiltration membranes: lateral migration and the particle trajectory model, *Desalination* 35 (1980) 129–147.
- [5] A.L. Zydney, C.K. Colton, A concentration polarisation model for the filtrate flux in crossflow microfiltration of particulate suspensions, *Chem. Eng. Commun.* 47 (1986) 1–21.
- [6] R.H. Davis, D.T. Leighton, Shear induced transport of a particle layer along a porous wall, *Chem. Eng. Sci.* 42 (2) (1987) 275–281.
- [7] M.R. Hoogland, A.G. Fane, C.J.D. Fell, The effect of pH on crossflow filtration of mineral slurries using ceramic membranes, in: *Proceedings of the First International Conference on Inorganic Membranes*, Montpellier, France, 1989, pp. 153–162.
- [8] V. Chen, A.G. Fane, S. Madaeni, I.G. Wenten, Particle deposition during membrane filtration of colloids: transition between concentration polarisation and cake formation, *J. Membr. Sci.* 125 (1997) 109–122.
- [9] J.A. Howell, Sub-critical flux operation microfiltration, *J. Membr. Sci.* 107 (1995) 165–171.
- [10] P. Bacchin, P. Airnar, V. Sanchez, Model for colloidal fouling of membranes, *AIChE J.* 41 (2) (1995) 368–376.
- [11] M. Hamachi, M. Mietton Peuchot, Experimental investigations of cake characteristics in crossflow microfiltration, *Chem. Eng. Sci.* 54 (1999) 4023–4030.